Supporting Information: Parallel polarization illumination with a multifocal axicon metalens for improved polarization imaging

Chen Chen[†, ‡, §, #], *Yiqun Wang*[†, ‡, §, #], *Minwei Jiang*[†, ‡, §], *Jian Wang*[†, ‡], *Jian Guan*[‡],

Baoshun Zhang[§], *Lei Wang*[‡], *Jie Lin*[†, ‡, *], *Peng Jin*[†, ‡, *]

[†] Key Laboratory of Micro-systems and Micro-structures Manufacturing, Ministry of Education, Harbin Institute of Technology, Harbin 150001, China

[‡] School of Instrumentation Science and Engineering, Harbin Institute of Technology, Harbin 150001, China

[§] Nanofabrication Facility, Suzhou Institute of Nano-Tech and Nano-Bionics, Chinese Academy of Sciences, Suzhou 215123, China

Table S1. Length (L) and width (W) of nanofins.

θ	0°		22.5°		45°		67.5°	
	W/nm	L/nm	W/nm	L/nm	W/nm	L/nm	W/nm	L/nm
#1	70	175	65	170	70	180	85	205
#2	80	175	75	180	80	185	55	185
#3	85	190	85	185	85	205	70	175
#4	90	210	90	205	55	200	80	180
#5	70	175	65	170	70	180	85	205
#6	80	175	75	180	80	185	55	185
#7	85	190	85	185	85	205	70	175
#8	90	210	90	205	55	200	80	180

The highlighted data means that the orientation angle for nanofins are θ+90°.

Table S2. Phase modulation precision of adopting the same/different nanofins.

	Phases of the same nanofins/degree				Phases of the different nanofins/degree			
θ	0°	22.5°	45°	67.5°	0°	22.5°	45°	67.5°
#1	-154.57	-147.44	-148.90	-148.69	-154.57	12.630	36.870	-57.420
#2	-110.84	-110.75	-110.20	-107.24	-110.84	54.090	81.480	-9.9000
#3	-68.78	-70.80	-70.72	-70.15	-68.780	106.01	122.89	32.560
#4	-20.58	-26.91	-28.74	-24.44	-20.580	151.66	176.97	77.130
#5	30.82	31.31	31.10	32.56	30.820	195.38	216.87	129.77
#6	74.06	72.76	69.80	69.25	74.060	239.47	261.48	171.11
#7	107.74	109.85	109.28	109.2	107.74	282.20	302.89	211.31
#8	160.52	155.56	151.26	153.09	160.52	327.08	356.97	256.56
MAD /degree	6.74				2.34			

1. The results listed in Table S2 demonstrate that optimizing extra 24 nanofins for three polarizations is higher phase modulation precision.

2. The phases of the same nanofins are simulated using 8 nanofins at different orientation angles, which are listed in the first column of Table S1. The phases of the

different nanofins are simulated using 32 nanofins at different orientation angles, which are listed in Table S1.

3. MAD, which means mean absolute deviation, is calculated as

$$\mathrm{MAD} = \frac{1}{32}\sum|(\varphi_s - \varphi_t)|,$$

$$\varphi_t(\theta,n) = \varphi_s(\theta,1) + (n-1)\cdot\frac{\pi}{4},$$

Where, φ_s is simulated phase; φ_t is target phase; θ is the orientation angle of nanofins; n represents n^{th} nanofin.

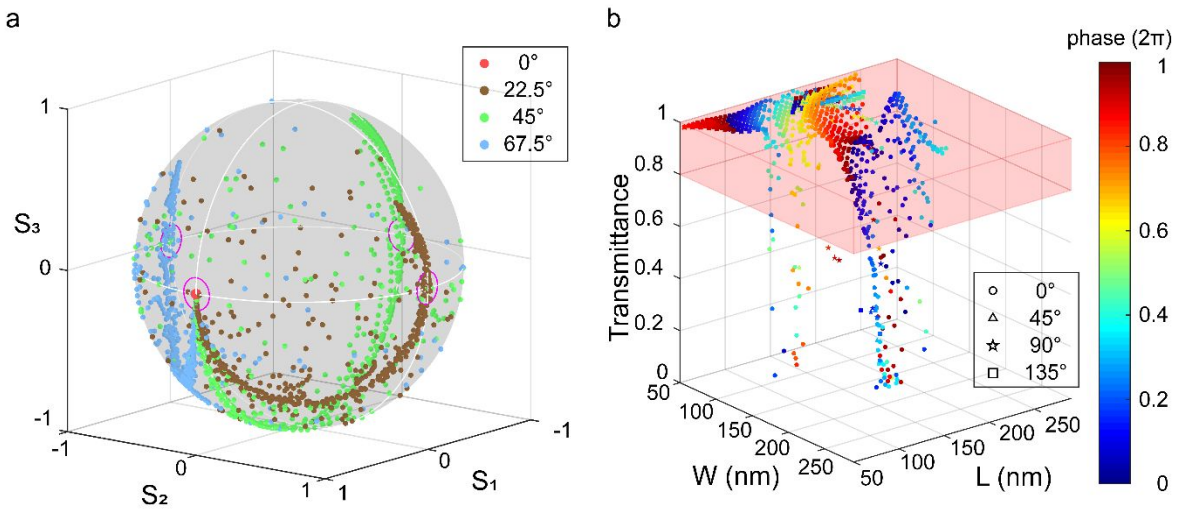

Figure S1. Simulated results of nanofins. (a) Polarization states of each nanofins on Poincare Sphere. The polarization states of nanofins rotated θ = 0°/22.5°/45°/67.5° are marked in red/yellow/green/blue dots. The points represent 0°/45°/90°/135° linear polarization located at (S_1, S_2, S_3) = (1, 0, 0), (0, 1, 0), (-1, 0, 0), and (0, -1, 0). The polarization states of 0° nanofins are all at the same point for 0° polarization. Other polarization states distribute at different points relying on varying *W* and *L*. The eligible nanofins are labeled in magenta circles. (b) Transmittance and phase of nanofins, which are chosen in Figure S1a. 0°/45°/90°/135° linear polarization are marked by circle/triangle/pentagram/square. High Transmittance and accurate phase value are considered in the optimization process.

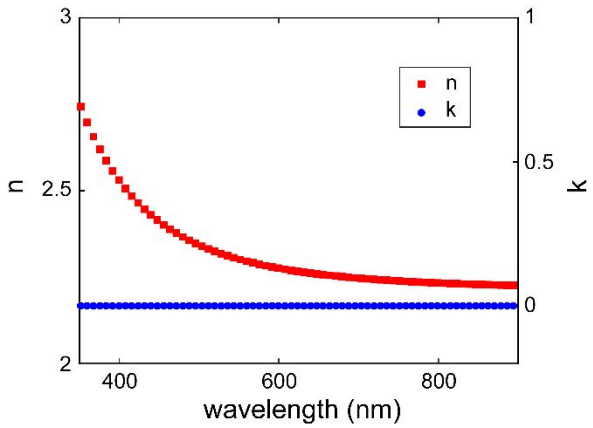

Figure S2. The n (red squares) and k (blue circles) of the refractive index. The data are obtained using an ellipsometer.

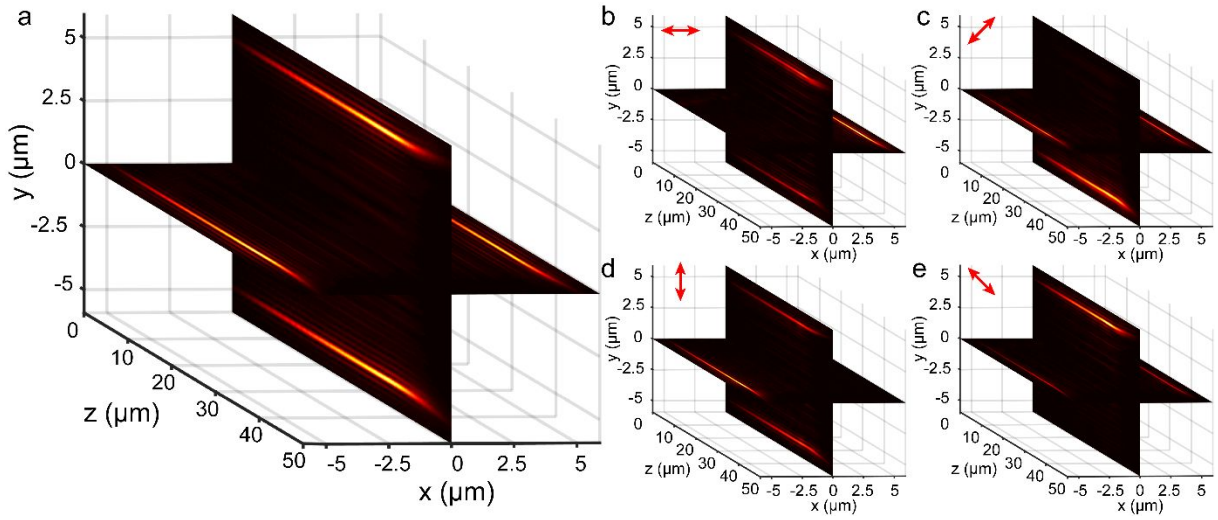

Figure S3. Measured three-dimension intensity-distribution of multifocal metalens (MFML) without polarizer (a) and with a polarizer along 0°/45°/90°/135° (b-e). The resolutions for *x*/*y*/*z* are 19.8/19.8/100 nm.

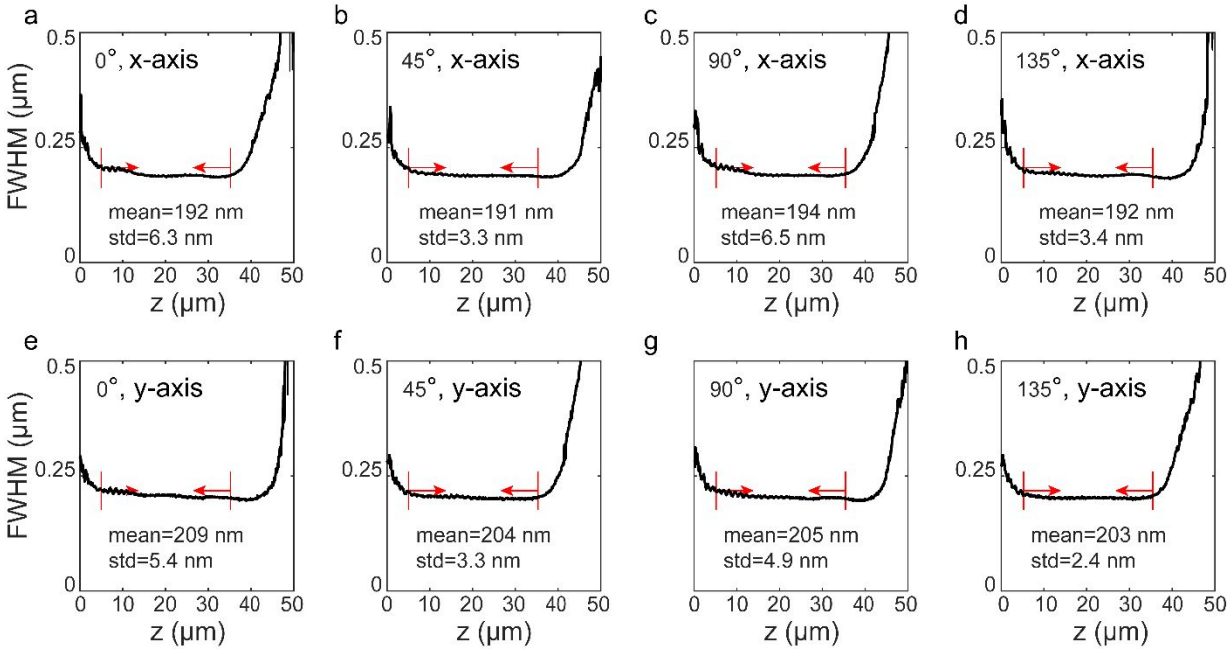

Figure S4. The full-widths at half-maximum (FWHMs) along the *x*-/*y*-axis for MFML as a function of *z*. The FWHM is obtained using Gaussian fitting. The mean and standard deviation (std) are labeled in corresponding figures. The spots in the range of z<5 μm are too weak to fit and the spots in the range of z>35 μm are diverging. Therefore, the range of 5–35 μm is using to calculate data. Besides, the means and standard deviations for four spots along the *x*-/*y*-axis are 192/205 nm and 5.2/4.7 nm. The mean and standard deviation for all spots are 199 nm and 8.1 nm.

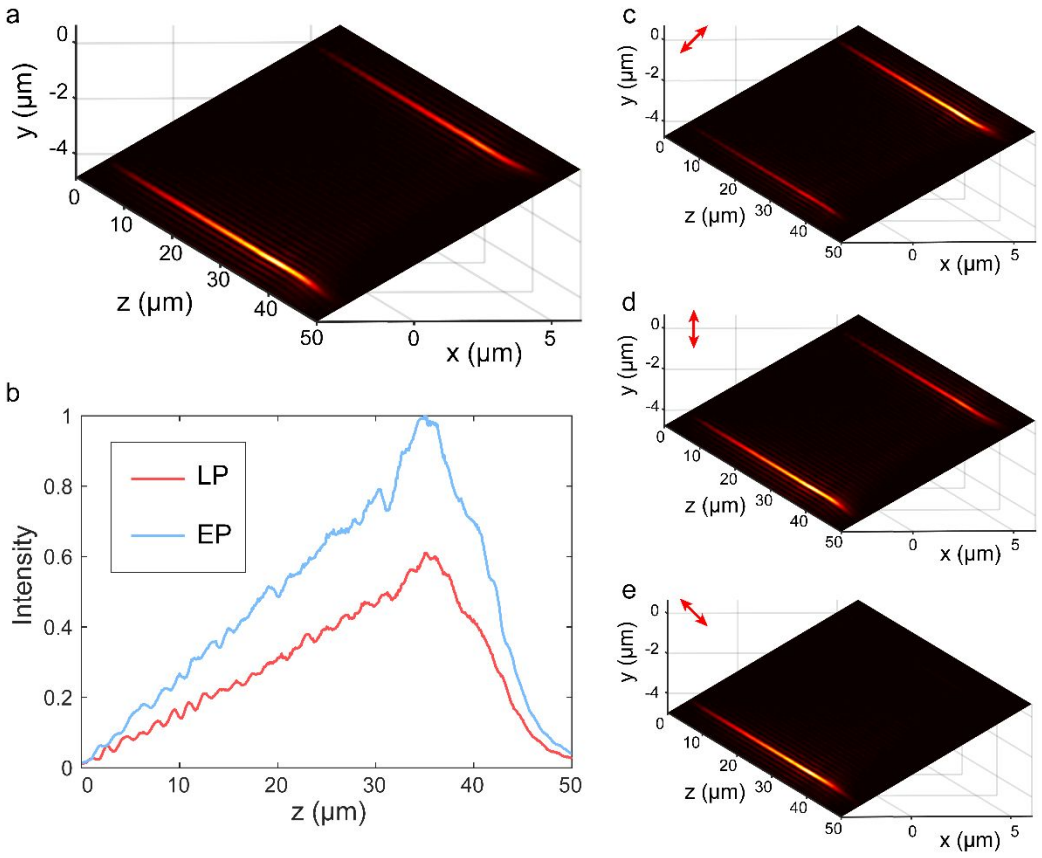

Figure S5. Measured intensity of double-focus metalens for elliptical polarization (DFML-EP). (a). Three-dimension intensity-distribution without polarizer. (b). Intensity profiles along the *z*-axis. The linear polarization (LP) and elliptical polarization (EP) are marked in red and blue. (c, d) Three-dimension intensity-distributions for the polarization components along 45°/90°/135°. The resolutions of *x*/*y*/*z* are 19.8/19.8/100 nm.

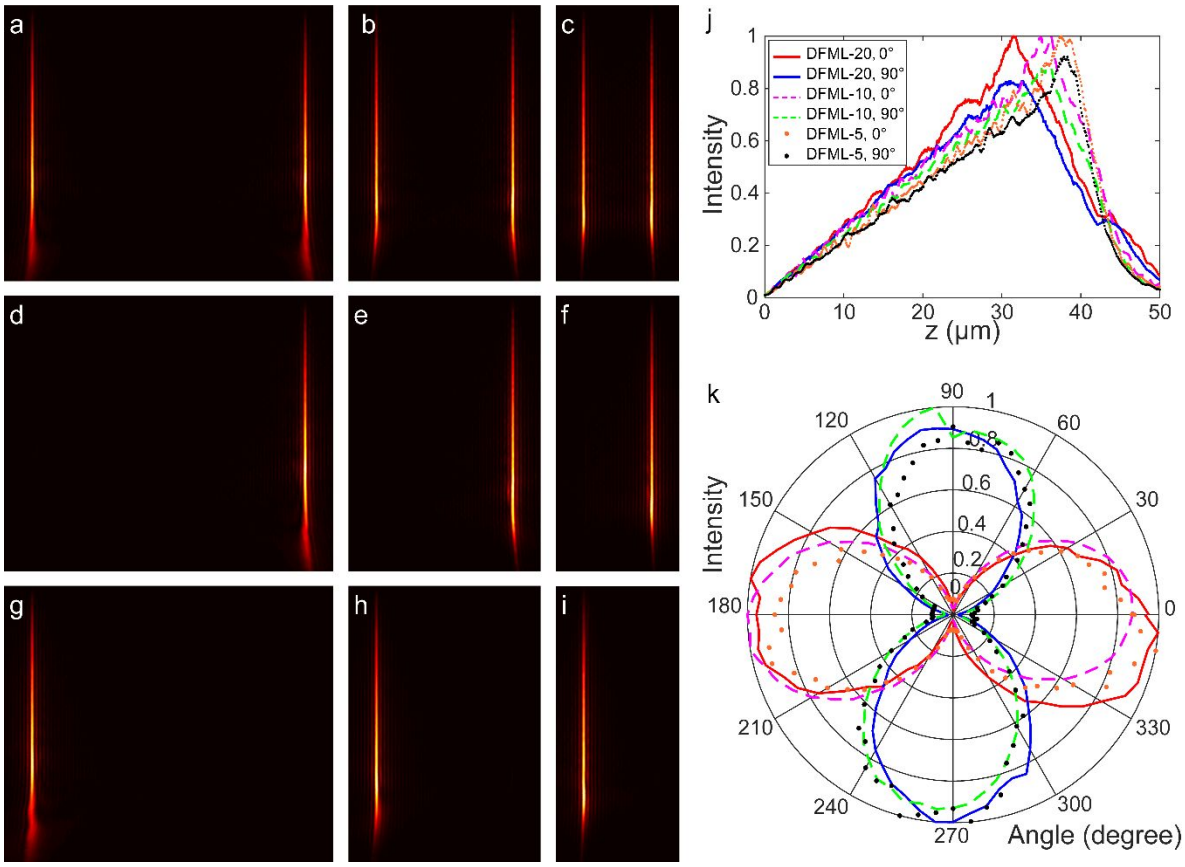

Figure S6. The measurement for a series of DFMLs with different distances between two spots which are 20 μm, 10 μm, and 5 μm respectively. The DFMLs are designed with R =49.92 μm and γ = 0.75. And the two spots are located on the x-axis symmetrically with x-/y-axis LP respectively. (a-i) The normalized intensity-distributions of DFML-20 (a, d, g), DFML-10 (b, e, h), and DFML-5 (c, f, i) at xz plane. (a-c) The total intensity without polarizer. (d-f) The intensity with a 0° polarizer. (g-i) The intensity with a 90° polarizer. Size: 23.76 μm ×50.1 μm, 13.88 μm ×50.1 μm, 8.93 μm ×50.1 μm. (j). Central intensity

profiles along the *z*-axis. The normalizing is acted on each DFML independently. The DFML-20, DFML-10, and DFML-5 are marked by line, dash, and dot. The 0° polarization and 90° polarization are marked in warm colors and cool colors. As the distance decreasing, the intensity uniformities for the two spots are ascending, which are 90.68%, 93.62%, and 95.93%. The average FWHMs for three devices keep consistent, which are 188 nm, 187 nm, and 189 nm with 3.1 nm, 2.4 nm, and 2.8 nm standard deviations. The DOFs are ascending, which are 32 μm, 36 μm, and 38 μm. The theoretical values are 35 μm, 40 μm, and 42 μm. It is worth noting that the lengths of total Bessel-beams are decreasing. The reason is that the tail is from the area exceeding R' which decreases with distance. (k) The states of polarization for six spots. The marks are the same as those in Figure S6j. The DOLPs of the two spots are (95.65%, 94.93%), (94.42%, 92.17%), and (87.11%, 83.49%), respectively. Becoming worse of DOLPs is caused by increased aliasing as distance decreases.

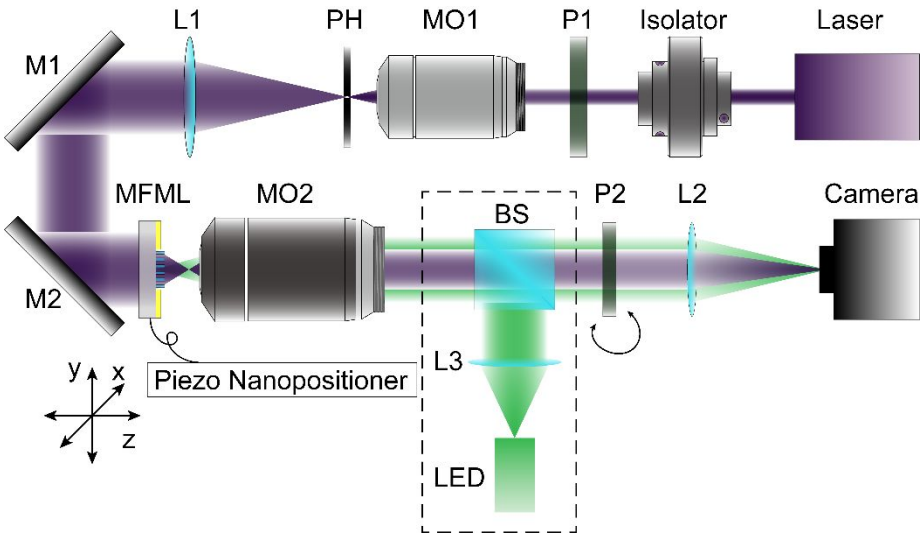

Figure S7. Optical experimental setup for field measurement. We replaced an opto-isolator (IO-3D-405-PBS, Thorlabs Inc.) and a polarizer (P1, 500:1) behind laser (OBIS 405 LX 50 mW, Coherent Inc.). Next, a filtering system, including an objective (MO1, 10x, NA = 0.25, Daheng Inc.), a 20 μm pinhole (PH), and a plano-convex lens (L1), was employed for a parallel and homogeneous beam which area is large enough. Veered though two dielectric mirrors (M1, M2, Edmund Inc.), incident beam injected perpendicularly onto the backside of the MFML mounted on a piezoceramic (P-733.3 XYZ Piezo Nanopositioner, PI Inc.). For imaging the optical field, we used a self-made microscope including an objective (MO2, MPLAPON100x, NA = 0.95, Olympus Inc.), a lens (L2, f = 200 mm) as the eyepiece, and a CMOS camera (MER-500-14U3M, pixel

size is 2.2 μm × 2.2 μm). The magnification of the microscope was 111 times approximately. Hence, a pixel on CMOS equaled to 19.8 nm correspondingly. During measuring, the MFML was drove along with the *z*-axis by piezoceramic with a step of 100 nm. Additionally, a polarizer (P2, 500:1) was inserted between objective and eyepiece for acquiring different components, and a LED source was introduced by a lens (L3) and a beam splitter prism for imaging our device.

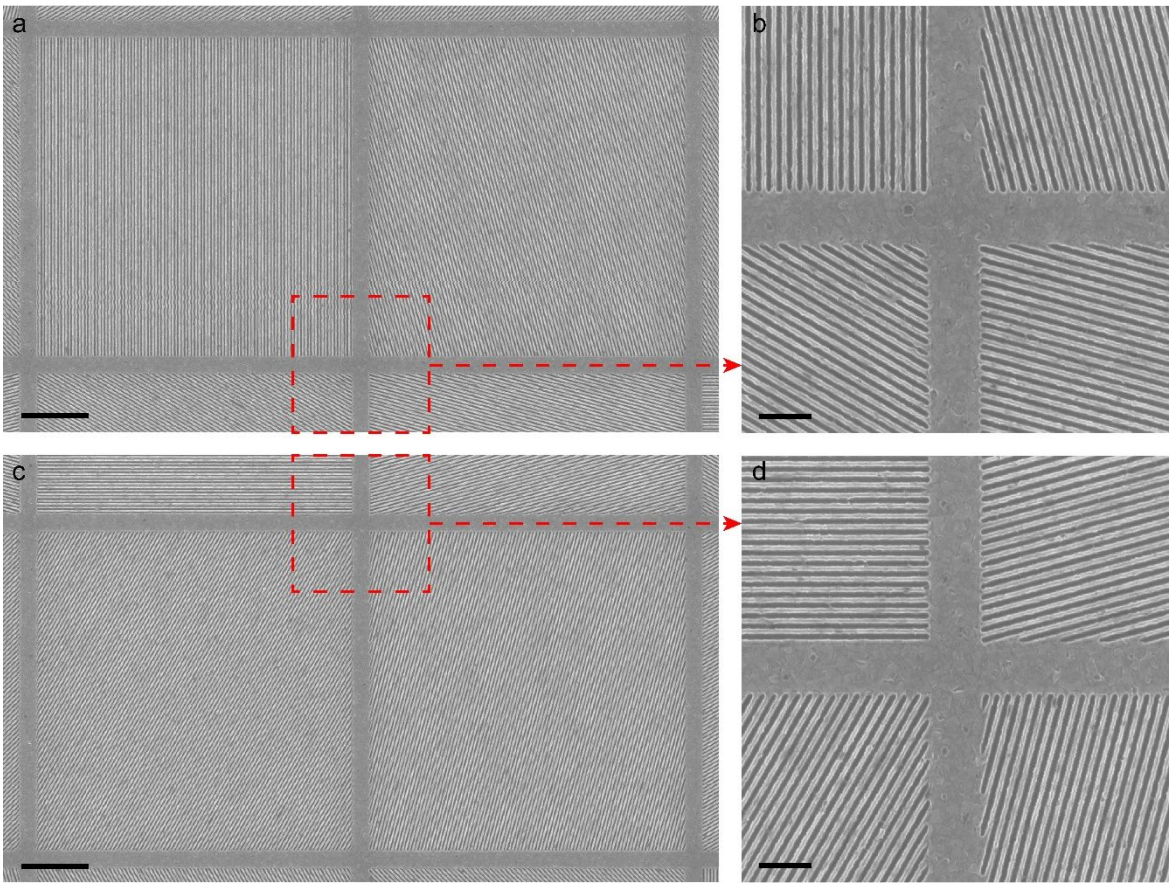

Figure S8. SEM images of aluminum grating. (a, c) Scale bar: 2 μm. (b, d) The magnifications of the dashed areas in (a, c). Scale bar: 500 nm. The sample is an aluminum grating on the SiO2 substrate which has many areas with different angles. Each grating area is 9.5 μm × 9.5 μm in size and arrays with a gap of 0.5 μm. There is a 15°-difference between the angles in adjacent areas. The grating is designed with a height of 100 nm and equal line widths/gaps of 50 nm. The grating is fabricated using electron beam lithography and metal dry etching.

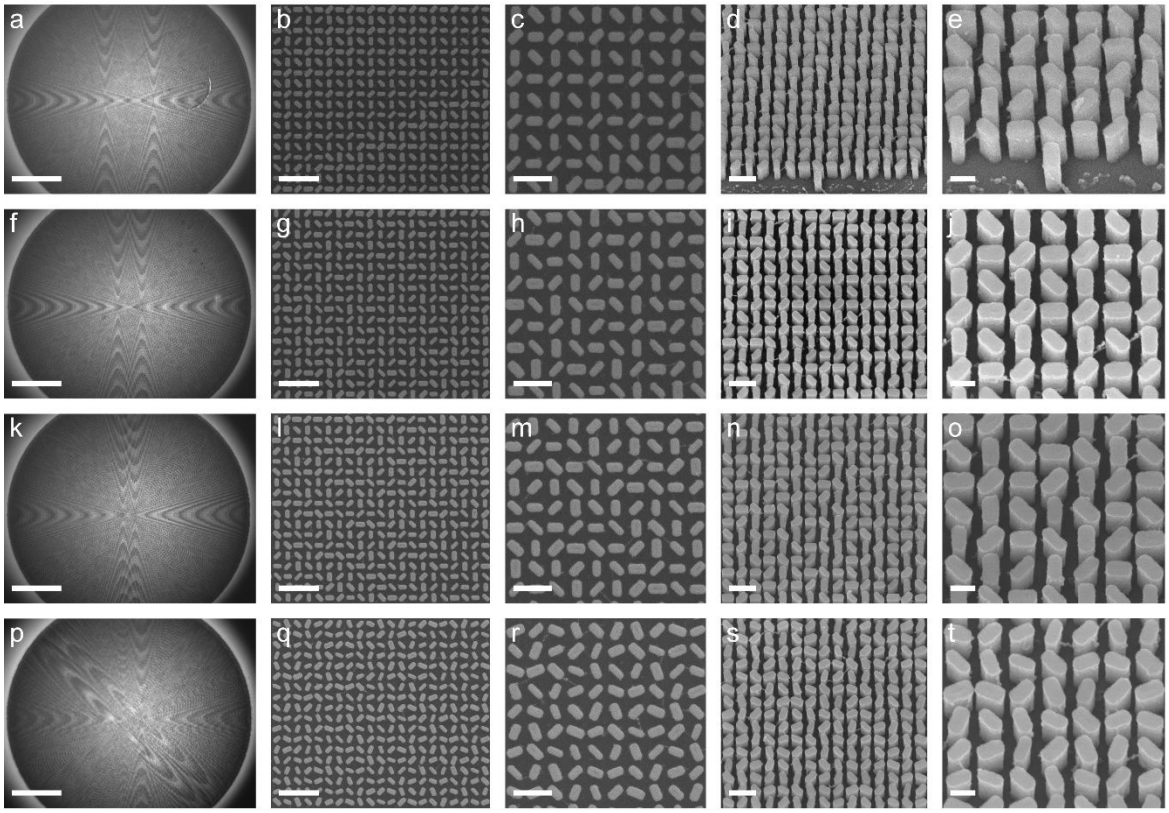

Figure S9. Optical microscope images (a, f, k, p) and SEM images (b-e, g-j, l-o, q-t) of DFML-20 (a-e), DFML-10 (f-j), DFML-5 (k-o), and DFML-EP (p-t). (a, f, k, p). Scale bar: 200 nm. (b, g, l, q). Scale bar: 1000 nm. (c, h, m, r). Scale bar: 500 nm. (d, i, n, s). Scale bar: 500 nm. (e, j, o, t). Scale bar: 200 nm.

Note S1. The calculation of polarization and intensity of EP.

The polarization of EP is calculated as

$$E_i = E_{90} + E_{135} = \begin{bmatrix} 0 \\ 1 \end{bmatrix} + \frac{\sqrt{2}}{2} \cdot \begin{bmatrix} -1 \\ 1 \end{bmatrix} \cdot e^{i\delta} = \begin{bmatrix} -\frac{\sqrt{2}}{2} e^{i\delta} \\ 1 + \frac{\sqrt{2}}{2} e^{i\delta} \end{bmatrix},$$

$$E_t(\varphi) = M_{\varphi - pol} \cdot E_i = \begin{bmatrix} \cos^2 \varphi & \sin \varphi \cos \varphi \\ \sin \varphi \cos \varphi & \sin^2 \varphi \end{bmatrix} \cdot \begin{bmatrix} -\frac{\sqrt{2}}{2} e^{i\delta} \\ 1 + \frac{\sqrt{2}}{2} e^{i\delta} \end{bmatrix},$$

$$I_t(\varphi) = E_t'^{*}(\varphi) \cdot E_t(\varphi),$$

Where E_{90} and E_{135} are Jones vectors of 90° and 135° polarization; δ = -1.65 rad is the phase difference between E_{90} and E_{135}; E_i and E_t are Jones vectors of light before and after a polarizer; $M_{\varphi\text{-}pol}$ is Jones matrix for a polarizer with an angle of φ; $I_t(\varphi)$ is measured intensity as a function of φ, which represents the polarization state for the spot; Symbol '' and '*' are transposition and conjugate.

The intensity of EP and the intensity ratio are calculated as,

$$I_{\mathrm{EP}} = E_i'^{*} \cdot E_i = 1.8881,$$

$$I_{\mathrm{LP}}{:}I_{\mathrm{EP}} = 1{:}1.8881 = 0.5296.$$

Note S2. The calculation for polarization angle.

The aluminum grating can work as polarizer. The Jones matrix of the sample is given as

$$M = R_\theta^{\mathrm{T}} M_x R_\theta = \begin{bmatrix} \cos\theta & -\sin\theta \\ \sin\theta & \cos\theta \end{bmatrix} \cdot \begin{bmatrix} \sqrt{t} & 0 \\ 0 & 0 \end{bmatrix} \cdot \begin{bmatrix} \cos\theta & \sin\theta \\ -\sin\theta & \cos\theta \end{bmatrix},$$

Where R_θ represents a rotation matrix; θ is the rotation angle; M_x is Jones matrix for a polarizer along the *x*-axis; *t* is the transmittance for the sample. The Jones vector of incident is supposed as $\begin{bmatrix} \cos\alpha \\ \sin\alpha \end{bmatrix}$, where α is the polarized angle for the incident. Therefore, the Jones vector for transmitted light is given as

$$E = M \cdot \begin{bmatrix} \cos\alpha \\ \sin\alpha \end{bmatrix} = \sqrt{t} \begin{bmatrix} \cos\theta\cos(\alpha-\theta) \\ \sin\theta\cos(\alpha-\theta) \end{bmatrix}.$$

The intensity for transmitted light is given as

$$I = \frac{1}{2} t(1 + \cos 2\alpha\cos 2\theta + \sin 2\alpha\sin 2\theta).$$

The α in our work can be expressed as $\alpha_i = i \cdot \frac{\pi}{4}$, *i* = 0, 1, 2, 3. Hence, a set of equations is given as

$$I_i = \frac{1}{2} t(1 + \cos 2\alpha_i\cos 2\theta + \sin 2\alpha_i\sin 2\theta).$$

As a solution of the equations, t and θ are written as

$$\begin{cases} t = 2 \cdot \sum_{i=0}^{N} \frac{1}{N} I_i \\ \tan 2\theta = \frac{\sum_{i=2k+1}^{N} (-1)^k I_i}{\sum_{i=2k}^{N} (-1)^k I_i}, \quad k = 0, 1, \ldots, \frac{N}{2} - 1 \end{cases}.$$